Co-published by
**Institute of Fluid-Flow Machinery**
Polish Academy of Sciences
**Committee on Thermodynamics and Combustion**
Polish Academy of Sciences



http://www.imp.gda.pl/archives-of-thermodynamics/

# Analysis of the accuracy of the inverse marching method used to determine thermal stresses in cylindrical pressure components

Magdalena Jaremkiewicz*

Cracow University of Technology, Faculty of Environmental and Energy Engineering, ul. Warszawska 24, Cracow 31-155, Poland
*Corresponding author email: magdalena.jaremkiewicz@pk.edu.pl

Received: 30.07.2024; accepted: 08.10.2024

## Abstract

This paper analyses the inverse marching method used to determine the thermal stresses on the inner surface of a thick-walled cylindrical element not weakened by holes in the transient state. The heat conduction problem was considered one-dimensional, i.e. it was assumed that heat is transferred only in the radial direction. The method is based on measuring the temperature inside the pipeline wall at a single point and assuming that the pipeline is thermally insulated. The paper undertook an evaluation of the influence of the measuring point's distance from the inner surface, the number of control volumes into which the inverted area was divided and the length of the time step on the accuracy of the calculated temperature, heat transfer coefficient and thermal stresses on the inner surface of the pressure element. Verification was performed by comparing the calculation results obtained from the direct analytical method perturbed by random errors with those obtained from the numerical inverse step method.

**Keywords:** Thermal stresses; Inverse heat conduction problem; Finite volume method

Vol. 45(2024), No. 4, 95–105; doi: 10.24425/ather.2024.152000

Cite this manuscript as: Jaremkiewicz, M. (2024). Analysis of the accuracy of the inverse marching method used to determine thermal stresses in cylindrical pressure components. *Archives of Thermodynamics*, 45(4), 95–105.

## 1. Introduction

The problem of identifying thermal stresses is essential in many different industries, such as conventional, nuclear, and renewable power generation, the metallurgical industry, the semiconductor industry, the automotive and aerospace industries, and even medicine.

One of the most popular methods for determining thermal stresses, as described in publications in recent years, is the finite element method (FEM). For example, for a case from the metallurgical industry considered in [1], the authors of the paper used FEM in the Ansys software to analyse the thermal stresses of a ladle refractory layer on molten steel. This analysis allowed the authors to evaluate the effect of dilatations of different sizes on the reduction of thermal stresses. Also, it allowed the creation of temperature and stress characteristics under different operating conditions.

In the context of conventional power generation, the unpredictability of renewable energy production results in the requirement for frequent start-up and shut-down and load shifting of power units. This results in a reduced equipment lifetime due to thermo-mechanical fatigue and creep. Monitoring power plant operating conditions and residual life assessments to ensure safe operation also requires power plants that have exceeded their design life. For the reasons mentioned above, correctly identifying the thermal stresses of critical pressure components of power

## Nomenclature

$a, b, c$ – coefficients of a polynomial function
$c$ – specific heat capacity, J/(kg K)
$E$ – Young's modulus, MPa
Fo – Fourier number
$h$ – heat transfer coefficient, W/(m$^2$K)
$k$ – thermal conductivity coefficient, W/(m K)
$\mathbf{K}$ – thermal conductivity tensor
$n_c$ – number of control volumes
$N$ – temperature measuring point
$p_n$ – overpressure of the fluid inside the cylindrical element, MPa
$\dot{q}_i$ – heat flux at the *i*-th node, W/m$^2$
$\dot{q}_v$ – energy generation rate per unit volume, W/m$^3$
$\dot{Q}_{i,j}$ – heat flow rate between the nodes *i* and *j*, W
$r$ – radius, m
$s$ – thickness, m
$s_{N,stresses}$ – mean squared error of thermal stresses, MPa
$s_{N,temp}$ – mean squared error of temperature, ºC or K
$t$ – time, s
$T$ – temperature, ºC or K
$T_i$ – temperature at the *i*-th node, ºC or K
$\bar{T}$ – average temperature over wall thickness, ºC or K
$v_T$ – rate of temperature change, K/s

### Greek symbols

$\alpha$ – stress concentration factor
$\beta$ – linear thermal expansion coefficient, 1/K
$\delta$ – distance from the internal surface to the measuring point, m
$\Delta r$ – spatial step, m
$\Delta t$ – time step, s
$\Delta V_i$ – volume of the *i*-th control cell, m$^3$
$\varepsilon$ – tolerance, K
$\kappa$ – thermal diffusivity coefficient, m$^2$/s
$\nu$ – Poisson's ratio
$\varrho$ – density, kg/m$^3$
$\sigma$ – circumferential stresses, MPa
$\phi$ – shape factor

### Subscripts and Superscripts

$al$ – allowable
$f$ – fluid
$in$ – inner
$m$ – mean
$out$ – outer
$p$ – caused by pressure
P – on the edge of the hole at point P
$T$ – thermal

### Abbreviations and Acronyms

FEM – finite element method
FVM – finite volume method
DCS – distributed control systems

boilers is crucial. Knowledge of the thermal stresses is also necessary for determining the optimum temperature histories of the fluid during heating [2] and cooling [3] of pressure components when the rate of temperature change is determined from the condition of not exceeding the allowable stresses.

Recently, many articles have been devoted to determining thermal stresses in nuclear power plants, where the issue of safe operation of pressure equipment is critical. An example is the paper [4], which presents a simplified method for determining thermal stresses at the corners of pressure vessel nozzles of nuclear reactors. In order to eliminate the disadvantage of the popular FEM method, i.e. the high computational cost for three-dimensional elements, the thermal stresses are estimated based on temperature gradients. Temperature gradients are predicted in the cross-section at the corners of the nozzles based on the known geometry of the element and the way the temperature is distributed in the cylindrical element and semi-infinite plate (determined analytically). The authors of the paper [5] also addressed the study of thermal stresses at the corners of reactor nozzles. They presented simple equations for the prediction of the stress intensity factor, which was obtained from thermal loading analysis under cooling and heating conditions using the FEM. The FEM analyses were used in both cases only to validate the proposed approach.

Residual stresses arising in pressure components due to thermal shock are also investigated. An example of research on this topic is the paper [6], where the authors characterised the residual stresses in a steel pressure vessel of a nuclear reactor whose surface is plated with a nickel-based alloy. The study's authors also investigated the interaction between residual and thermal stresses during thermal shock.

A common area for conventional and nuclear power plants with a high need for thermal stress analysis are steam turbines. In [7], an algorithm for monitoring thermal stresses in rotors and bodies of shut-off and control valves of steam turbines is presented. The developed software allows the determination of stresses in critical turbine components based on measured data, and it will also enable the optimisation of the device start-up process. In [8], thermal stresses were analysed for the case of high-temperature steam inlet to steam turbines with a combined HP-IP cylinder and high- and medium-pressure rotors located in separate casings, operating with a double or single thermal bypass. On the other hand, in [9], acceptable parameter deviations were analysed to assess the quality of the start-up operation in terms of the thermal stress values of the critical elements of the power plant thermal scheme, i.e. the high-pressure turbine rotor and the high-pressure outlet header of the recovery boiler superheater. Calculations were performed using the Ansys software.

Determining thermal stresses in a thick-walled element without holes, in both quasi-stationary and transient states, requires knowledge only of the temperature distribution in the wall of the element. However, thick-walled elements often have holes, and a quasi-stationary state is difficult to achieve in practice. Given this, the thermal stresses can only be correctly calculated by knowing the stress concentration factor at the edge of the hole and, in turn, this without knowing the exact temperature of the fluid flowing through the element and the heat transfer coefficient at its internal surface.

In order to determine the heat transfer coefficient, exact transient temperature measurements are required due to the slight difference between the fluid temperature at high pressure and the internal surface temperature of the component. The heat

transfer coefficient has an essential influence on the optimum rate of change of the fluid temperature, which is determined by the condition of not exceeding the allowable thermal stresses on the inner surface of the pressure element [10]. Strain and stress analyses demonstrate that the influence of the time- and location-varying heat transfer coefficient compared to the fixed coefficient recommended by standards is a crucial factor in fatigue calculations. The importance of determining the actual heat transfer coefficient on the internal surface of pressure components based on numerical studies of steam boiler start-up and analysing deformations and stresses in the component is demonstrated in [11].

The highest thermal stresses occur on the inner surface of the pressure element, which is in direct contact with the high-pressure, high-temperature fluid. In order to determine the stresses on this surface, a temperature measurement is usually taken in practice at half the wall thickness s and a distance δ from the inner surface of the element of 6 to 10 mm [12]. This method in transient states is characterised by low accuracy. The stresses on the inner surface of the element determined in this way may differ by up to several tens per cent from the actual stresses, significantly when the steam temperature changes rapidly.

An attempt to develop a mathematical model using the finite difference method to determine the transient thermal stresses in a thick-walled pressure component was made in the article [13], among others. The developed model has been verified experimentally and compared to a model based on FEM. The model uses known temperatures of the surroundings, external surface and fluid inside the cylindrical element. The method considered is based on solving a direct problem.

Another approach to determining transient thermal stresses based on the temperature distribution inside the wall of a pressure element is to use methods based on solving the inverse heat conduction problem [14]. In the inverse heat conduction problem, the temperature at the edge of the element is determined based on temperature changes at selected points inside the analysed body. The determination of thermal stresses based on the measurement of the wall temperature of a thick-walled element with simple shapes near the inner surface is presented in the article [12]. The temperature measurement location divides the wall in the cross-section into direct and inverse areas, with the finite volume method (FVM) being used in the inverse area to determine the temperature distribution and heat flux. Knowing the heat flux and temperature at the internal surface and the temperature of the fluid washing over this surface allows the heat transfer coefficient to be determined. The technique of measuring the fluid temperature with new solid-sheathed thermometers using the inverse solution of the heat conduction problem is described in detail in [15]. In turn, papers [16,17] present a method for determining the three-dimensional temperature field in thick-walled elements based on temperature measurements at a series of points on the thermally insulated external surface. In [16], a flat element was analysed and in [17], a cylindrical one. In addition, a method for determining the heat transfer coefficient has been developed for the case of an element with complex shapes. This method is made possible by a 'measuring probe', by which the temperature is measured at 6 points near the inner surface of the component [18].

Inverse problems are characterised by a high sensitivity of the solution to input disturbances. To reduce their influence on the solution of the inverse problem, one of the regularisation methods, such as the Tikhonov method, discrete Fourier transform, energy regularisation method and others, can be used. Examples of research on Tikhonov regularisation and its modifications are presented in papers [19,20]. The paper [19] investigated the solution of an inverse problem illustrating the wall of a heating device, in which the regularisation parameter was chosen based on Morozov's principle. The paper [20], on the other hand, analysed the effect of the regularisation of the inverse problem on the stability of the calculated boundary conditions during the cooling of a sample in a thermo-chemical treatment furnace. A slightly different approach is proposed in [21], for the analysis of a ceramic-coated metal element (e.g. a turbine blade), where the temperature of the metal is controlled by solving the Cauchy problem for the heat conduction equation for a two-layer element. A regularisation method based on the energy balance formulation for the ceramic layer was used here, and the spectral radius of the equation matrix was used to analyse the stability of this computational model.

Another effective and simple solution that eliminates the influence of random errors on computational results in solving inverse problems and that can be applied in real time is smoothing measurement data by approximating the measured values with digital filters [22]. The smoothing of $N$-measured data in the form $f_s = f(s)$ is implemented by the least squares method using orthogonal Gram polynomials. An example of the use of digital filters for smoothing measured data is presented in the paper [15], which demonstrates the application of a new measurement technique to determine the transient temperature of superheated steam flowing out of the second superheater stage in a power boiler, based on the solution of an inverse problem.

This paper undertakes the determination of thermal stresses in thick-walled pressure elements using an inverse method based on FVM. The case of a transient and a cylindrical element not weakened by holes is considered. While the method is well-known and, for a cylindrical element, has been described in works [12,14], this article focuses on determining the best conditions for its application. The analysis of the accuracy of the inverse method consisted of selecting the most favourable division into control volumes depending on the distance of the temperature measuring point from the inner surface and the length of the time step. This was possible based on the computational tests performed, which made it possible to compare the determined temperature distribution and thermal stresses on the inner surface determined by the analytical method and the direct solution of the heat conduction problem with the results obtained from the inverse solution. The choice of the inverse method to determine the temperature distribution for thermal stresses using the control volume method to carry out accuracy analyses and conditions of applicability was due to a number of its advantages. Its use is simple in practice and does not require temperature measurements to be taken on the internal surface of pressure parts, especially as this would be very difficult in the

case of pressurised components. Furthermore, the method can be used for online stress monitoring. As described in this chapter, FEM for determining stresses is very popular. However, it requires the solution of a direct problem and, in the case of components with complex shapes, consumes a large amount of computational cost.

## 2. Determination of thermal stresses on the inner surface of pressure elements

Thick-walled components are used in power plant units due to the high pressure of the working fluid. The highest thermal stresses in thick-walled pressure components usually occur when there is a change in temperature during operation with a simultaneous uneven temperature distribution at the cross-section of the component walls, i.e. during start-up and shut-down. As a result of the standardisation of calculation procedures for boilers, the German regulation TRD 301 [23] and the European standard EN 12952-3 [24] were developed. These are the essential documents describing procedures for determining thermal stresses in pressure components. However, they are limited only to determining thermal stresses under the assumption of a quasi-stationary temperature field in the element wall, which is difficult to achieve in practice. Also, the assumption of a parabolic temperature distribution in the wall does not give satisfactory results for rapid and sudden temperature changes over time.

Simplified methods for determining transient thermal stresses on the surfaces of pressure parts washed with a working fluid based on the provisions mentioned above are described below. The main advantage of the methods discussed in this section is the simple formulae for determining the stresses on the inner surface of the element. Despite their approximate nature, they are used by boiler manufacturers. However, due to the development of DCS (distributed control systems) in power plants, there is now the possibility of using more complex formulas to calculate stresses online.

### 2.1. Thermal stresses in the plate assuming a quasi-stationary temperature field

Cylindrical pressure elements with a large diameter can be treated as flat elements. It is then assumed that the element can expand freely but not bend. An example of a cylindrical element that can be treated as a flat wall is the wall of a steam drum.

The basis for determining allowable heating and cooling rates of thick-walled cylindrical pressure elements is the condition of not exceeding the circumferential allowable stresses on the inner surface of the pressure element at the hole's edge at point P. The circumferential stresses at point P are the sum of the stresses due to pressure and thermal stresses:

$$\sigma_{\mathrm{P}} = \alpha_p \sigma_p + \alpha_T \sigma_T, \tag{1}$$

where $\alpha_p$ is the pressure stress concentration factor at point P lying on the edge of the hole (Fig. 1), and $\alpha_T$ is the thermal stress concentration factor at point P.

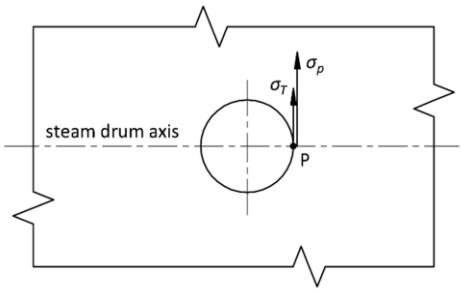


Fig. 1. Section of the wall of a steam drum with a hole.

The symbol $\sigma_p$ denotes the circumferential stresses from the pressure in a cylindrical element not reinforced by holes, which are expressed by the relation:

$$\sigma_p = \frac{p_n r_m}{s}, \tag{2}$$

where $p_n$ is the overpressure of the medium inside the element, $s$ is the thickness of the element, and $r_m = (r_{in} + r_{out})/2$ is the mean radius of the cylindrical pressure element determined as the arithmetic mean of the inner radius $r_{in}$ and the outer radius $r_{out}$.

The highest thermal stress in a cylindrical element occurs at the surface in contact with the fluid and is determined by the formula:

$$\sigma_T = \frac{E\beta}{1-\nu}\left(\bar{T} - T|_{r=r_{in}}\right), \tag{3}$$

where $E$ is Young's modulus, $\beta$ is the linear thermal expansion coefficient, $\nu$ is Poisson's ratio, $T$ is the temperature, and $\bar{T}$ denotes the average temperature over wall thickness.

After determining the average wall temperature of the component $\bar{T}$ from the solution of the heat conduction equation, a general relationship is obtained:

$$\sigma_T = \phi \frac{E\beta}{1-\nu}\frac{v_T s^2}{\kappa}, \tag{4}$$

where the symbol $\phi$ is usually referred to as the shape factor, $\kappa$ is the thermal diffusivity coefficient, and $v_T$ is the rate of temperature change.

For the inner surface of a cylinder, the ends of which are free to extend, the shape factor for a cylindrical element [24,25] is expressed by the formula:

$$\phi = \frac{1}{8}\frac{(k^2-1)(3k^2-1)-4k^4 \ln k}{(k^2-1)(k-1)^2}, \tag{5}$$

where $k = r_{out}/r_{in}$.

Stress concentration factors can be determined based on EN 12952-3 [24] or can be determined by FEM in the case of vessel-to-spigot connections with more complex geometries. The allowable heating or cooling rates of a pressure element are determined by the condition:

$$\sigma_{\mathrm{P}} \leq \sigma_{al}, \tag{6}$$

where $\sigma_{al}$ is the allowable stress determined from the Wöhler fatigue diagram in the standard [24].

Equation (6) gives satisfactory results when determining the permissible heating rates from the cold state when the pressure element is heated at a constant rate over a long time. With a time-varying rate of change in the fluid temperature, Eq. (1) is not very accurate, particularly with rapid temperature changes. Sudden changes in the fluid temperature occur, for example, when the evaporator is flooded with hot water at the beginning of a start-up, when cooling water is injected in superheated steam temperature controllers or when the boiler pressure is suddenly reduced due to damage to the steam evaporator tubes or superheaters.

It should be added that Eq. (1) remains valid at the pressure elements for time-varying heating or cooling rates.

This paper focuses only on the determination of thermal stresses.

### 2.2. Transient thermal stresses in a cylindrical element

A more general method for determining the thermal stresses in cylindrical elements without holes is the one using Eq. (3), where the average temperature $\bar{T}$ over the wall thickness is determined from the formula:

$$\bar{T} = \frac{2}{r_{out}^2 - r_{in}^2} \int_{r_{in}}^{r_{out}} rT(r,t)dr, \tag{7}$$

where $r$ denotes the radius.

The spatiotemporal distribution of the temperature in a cylindrical wall can be obtained from the analytical solution of the heat conduction equation or by using numerical methods, for example FEM or FVM. When numerical methods are used, the wall temperature is determined only at discrete points, while the average temperature is determined using the chosen approximation method [26,27]. By calculating the integral in Eq. (7) using, for example, the trapezoidal rule for discrete points, the following expression is obtained:

$$\bar{T} = \frac{1}{r_{out}^2 - r_{in}^2} \sum_{i=2}^{N} (r_{i-1}T_{i-1} + r_i T_i)\Delta r, \tag{8}$$

where $r_i$ is the radius at which the $i$-th node is located, $\Delta r$ is the spatial step, and $T_i$ is the temperature at the $i$-th node.

In some cases, the number of points at which the wall temperature is determined may be too small, and the accuracy of the average temperature determined from Eq. (8) may be insufficient. Another method of determining the average wall temperature can then be used, in which temperatures determined, for example, from the inverse solution of the heat conduction equation are interpolated by a second-degree polynomial [26,27]:

$$T(r,t) = a(t) + b(t)r + c(t)r^2, \tag{9}$$

where $a(t)$, $b(t)$ and $c(t)$ denote time-dependent coefficients.

For example, if the temperature is measured at two points in the wall, i.e. $T_1$ at the inner radius $r_{in}$ and $T_2$ at half the wall thickness at radius $r_m$, and the pipeline is insulated at the outer surface, after determining the coefficients $a(t)$, $b(t)$ and $c(t)$ for such boundary conditions and substituting the resulting temperature distribution $T(r,t)$ expressed by Eq. (9) into Eq. (7), the following relation is obtained:

$$\bar{T} = T_1 + \frac{2}{9}\left(4 + \frac{\Delta r}{r_{in}+\Delta r}\right)(T_2 - T_1). \tag{10}$$

Both Eqs. (8) and (10) make it possible to calculate the approximate value of the average temperature over the thickness of the cylindrical wall.

## 3. Determination of the one-dimensional temperature distribution in a cylindrical element using the inverse marching method

Suppose the temperature measurement in the thick-walled component can only be realised at the external surface and/or inside the pipe wall. In that case, the transient temperature field in the inverse region can be determined from the solution of the inverse heat conduction problem.

The general form of the heat conduction equation for stationary solids that can be treated as incompressible is presented as follows [28]:

$$c(T)\rho(T)\frac{\partial T}{\partial t} = \nabla(\mathbf{K}\nabla T) + \dot{q}_v, \tag{11}$$

where $c$ is the specific heat capacity, $\rho$ is the density, $\mathbf{K}$ is the thermal conductivity tensor, and $\dot{q}_v$ is the energy generation rate per unit volume.

In [28], FVM was used to solve the inverse problem: the heat conduction equation and known boundary conditions. FVM, also known as the control volume method, is versatile and efficient for solving heat conduction problems. Assuming that the temperature field is two-dimensional and the physical properties: specific heat capacity $c$, density $\rho$, thermal conductivity coefficient $k$ and energy generation rate per unit volume $\dot{q}_v$ are temperature dependent, the heat conduction equation can be transformed to the form:

$$\Delta V_i c(T_i)\rho(T_i)\frac{\partial T_i}{\partial t} = \sum_{j=1}^{n_c} \dot{Q}_{i,j} + \Delta V_i \dot{q}_v(T_i), \tag{12}$$

where $\dot{Q}_{i,j}$ is the heat flux rate transferred from node $j$ inside the neighbouring cell to node $i$, and $\Delta V_i$ is the volume of the $i$-th control cell. Node $i$ is located inside the analysed area and heat transfer occurs in $n_c$ control volumes adjacent to the analysed control area.

In this paper, the inverse heat conduction problem will be solved for the case of a cylindrical wall when heat is transferred only in the radial direction.

The proposed inverse method is stable and has high accuracy if the condition is met [29]:

$$\Delta \mathrm{Fo} \geq 0.05. \tag{13}$$

Furthermore, due to the method's sensitivity to random errors in the temperature measurement $T(t)$, to at least partially eliminate their influence on the calculation results, the temperature waveform is proposed to be smoothed using a 9-point digi-

tal filter [22]. Filtering also makes it possible to accurately determine the values of the derivatives of the temperature function $T(t)$ from measured data perturbed by random errors.

### 3.1. One-dimensional transient temperature field in elements with simple shapes

In the measurement method, the temperature, heat transfer coefficient and thermal stresses on the inner surface of a thick-walled cylindrical element are determined by measuring the temperature inside the wall at a single point. For this purpose, the temperature distribution in the area $r_{in} \le r \le r_{out}$ and the heat flux density on the pipe's inner surface are investigated. The temperature measurement is taken at node *N* inside the pipe wall, which has been thermally insulated (Fig. 2). The pipeline cross-section is divided into a direct and an inverse region, where the boundary between the two is at radius $r_N$.

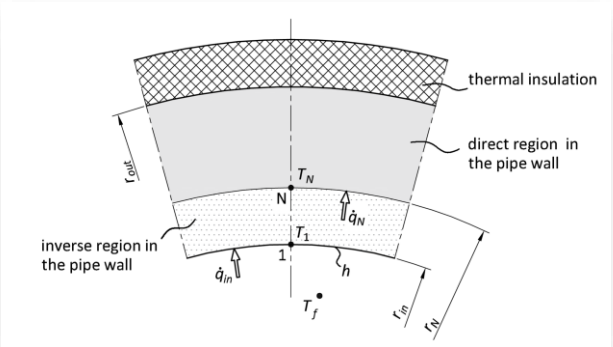


Fig. 2. Pipe wall cross-section with control volumes.

Heat transfer through the cylindrical wall is assumed to take place only in the radial direction $r$. In this case, the heat conduction equation in the cylindrical coordinate system takes the form [29,30]:

$$c(T)\rho(T)\frac{\partial T}{\partial t} = \frac{1}{r}\frac{\partial}{\partial r}\left[k(T)r\frac{\partial T}{\partial r}\right]. \tag{14}$$

The heat conduction equation is solved first for the direct area for the boundary conditions:

$$T|_{r=r_N} = T_N, \tag{15}$$

$$k(T)\frac{\partial T}{\partial r}\Big|_{r=r_{out}} = 0, \tag{16}$$

where $T_N$ is the temperature measured at node *N* located inside the pipeline wall (Fig. 2). In this way, the temperature distribution in the area $r_N \le r \le r_{out}$ and the heat flux $\dot{q}_N$ at node *N* are determined. The solution assumes that the values of the physical properties of the pipe material: $c, \rho, k$ are variable and temperature dependent.

Equation (14) is then solved for the inverse region $r_{in} \le r \le r_N$ using the boundary conditions:

$$T|_{r=r_N} = T_N, \tag{17}$$

$$k(T)\frac{\partial T}{\partial r}\Big|_{r=r_N} = \dot{q}_N. \tag{18}$$

The inverse problem described by Eqs. (14) and (16)–(18) was solved using FVM (Eq. (12)) and approximating the derivatives of the temperature function by differential quotients:

$$\frac{\partial T}{\partial r}\Big|_{r_{i+1}} = \frac{T_{i+1}-T_i}{\Delta r}, \quad \frac{\partial T}{\partial r}\Big|_{r_i} = \frac{T_i-T_{i-1}}{\Delta r}. \tag{19}$$

An illustration of the division of the inverse area into control volumes is shown in Fig. 3. As for the direct area, this solution assumes that the values of the physical properties of the pipe material $c$, $\rho$, $k$ are temperature-dependent. FVM allows the temperature distribution in the area $r_{in} \le r \le r_N$ to be determined. Some examples of the division of the inverse area into different numbers of control volumes are shown in Fig. 3.

The energy balance equation for the control volume with node *N* has the form:

$$\pi\left[{r_N}^2 - \left(r_N - \frac{\Delta r}{2}\right)^2\right]c(T_N)\rho(T_N)\frac{dT_N}{dt} =$$
$$= 2\pi\left(r_N - \frac{\Delta r}{2}\right)\frac{k(T_{N-1})+k(T_N)}{2}\frac{T_{N-1}-T_N}{\Delta r} + 2\pi r_N\dot{q}_N, \tag{20}$$

from which the temperature $T_{N-1}$ can be determined:

$$T_{N-1} = \frac{(\Delta r)^2\left(r_N-\frac{\Delta r}{4}\right)}{r_N-\frac{\Delta r}{2}}\frac{c(T_N)\rho(T_N)}{k(T_{N-1})+k(T_N)}\frac{dT_N}{dt} +$$
$$-\frac{2r_N\Delta r}{r_N-\frac{\Delta r}{2}}\frac{\dot{q}_N}{k(T_{N-1})+k(T_N)} + T_N. \tag{21}$$

The energy balance equation for a full-dimensional control volume (with thickness $\Delta r$) for nodes 2 to $(N-1)$ is shown in the following equation:

$$\pi\left[\left(r_{in}+(2i-1)\frac{\Delta r}{2}\right)^2 - \left(r_{in}+(2i-3)\frac{\Delta r}{2}\right)^2\right]\times$$
$$c(T_i)\rho(T_i)\frac{dT_i}{dt} = 2\pi\left(r_{in}+(2i-3)\frac{\Delta r}{2}\right)\frac{k(T_{i-1})+k(T_i)}{2}\frac{T_{i-1}-T_i}{\Delta r} +$$
$$+2\pi\left(r_{in}+(2i-1)\frac{\Delta r}{2}\right)\frac{k(T_i)+k(T_{i+1})}{2}\frac{T_{i+1}-T_i}{\Delta r},$$
$$i = 2,\dots,N-1, \tag{22}$$

from which the temperature $T_{i-1}$ can be determined:

$$T_{i-1} = 2(\Delta r)^2\frac{2r_{in}+(2i-2)\Delta r}{2r_{in}+(2i-3)\Delta r}\frac{c(T_i)\rho(T_i)}{k(T_{i-1})+k(T_i)}\frac{dT_i}{dt} +$$
$$-\frac{2r_{in}+(2i-1)\Delta r}{2r_{in}+(2i-3)\Delta r}\frac{k(T_i)+k(T_{i+1})}{k(T_i)+k(T_{i-1})}(T_{i+1}-T_i) + T_i. \tag{23}$$

Since for individual temperatures $T_{i-1}$ (for $i = 2,\dots,N$) the values of $k(T_{i-1})$ are not known (the equation is non-linear), the sought temperature $T_{i-1}$ is obtained after *n* iterations. In the first iteration $(n=0)$ for individual nodes, it is assumed that $k\left(T_{i-1}^{(0)}\right) = k(T_i)$.

The iteration process continues until a condition is met [29]:

$$\left|T_{i-1}^{(n+1)} - T_{i-1}^{(n)}\right| \le \varepsilon, \tag{24}$$

where the tolerance $\varepsilon \approx 0.000\,01$ K. If the values of the physical properties are constant, iterations are not required.

FVM also allows the heat flux $\dot{q}_{in}$ at the inner surface of the pipeline to be determined from the energy balance for node 1:

$$\pi\left[\left(r_{in}+\frac{\Delta r}{2}\right)^2-r_{in}^2\right]c(T_1)\rho(T_1)\frac{dT_1}{dt}=$$
$$=2\pi r_{in}\dot{q}_{in}+2\pi\left(r_{in}+\frac{\Delta r}{2}\right)\frac{k(T_2)+k(T_1)}{2}\frac{T_2-T_1}{\Delta r}, \quad (25)$$

from which it can be determined:

$$\dot{q}_{in}=\frac{\left(r_{in}+\frac{\Delta r}{2}\right)^2-r_{in}^2}{2r_{in}}c(T_1)\rho(T_1)\frac{dT_1}{dt}+$$
$$-\frac{k(T_2)+k(T_1)}{2}\frac{r_{in}+\frac{\Delta r}{2}}{r_{in}\Delta r}(T_2-T_1). \quad (26)$$

The application of the described method in the inverse region consists in determining the temperatures at successive nodes ($(N-1)$, $(N-2)$,..., 2 and 1) marching towards the inner surface of the pipeline. Based on the measured temperature $T_N(t)$ inside the pipeline wall at node $N$, the temperature of node $(N-1)$ is determined from Eq. (21). If the solution of the direct problem allows this and the temperature at node $(N+1)$ is calculated, the temperature at node $(N-1)$ can be determined from Eq. (23). By substituting the calculated temperature $T_{N-1}(t)$ into Eq. (23), the temperature $T_{N-2}(t)$ at node $(N-2)$ is determined. The procedure is repeated using Eq. (23) until the temperature $T_1(t)$ at node 1 is determined. Knowing the temperatures $T_1(t)$ and $T_2(t)$ from Eq. (26) the heat flux $\dot{q}_{in}(t)$ on the inner surface of the pipe can be determined.

In order to determine the heat transfer coefficient at the internal surface of the pipe $h$, it is necessary to know the temperature of the fluid $T_f$ flowing through the pipe. The boundary condition should then be used:

$$\dot{q}|_{r=r_{in}}=h\left(T_f-T|_{r=r_{in}}\right), \quad (27)$$

where

$$T|_{r=r_{in}}=T_1,\ \dot{q}|_{r=r_{in}}=\dot{q}_{in}. \quad (28)$$

A transformation of Eq. (27) gives:

$$h=\frac{\dot{q}_{in}}{T_f-T_1}. \quad (29)$$

After determining the temperature distribution at the cross-section of the cylindrical element at time $t$, the temperature distribution at time $t+\Delta t$ is calculated.

## 4. Computational validation of the inverse method

The calculations were carried out for a header with an external diameter of 355 mm and a wall thickness of 50 mm. The pipe material is P91 steel. The temperature-dependent physical properties of the steel were assumed for the calculations:

$$k(T)=-0.003\times10^{-10}T^5+4.741\times10^{-10}T^4+$$
$$-2.874\times10^{-7}T^3+6.438\times10^{-5}T^2+$$
$$-4.177\times10^{-4}T+28.676, \quad (30)$$

$$c(T)=1.41\times10^{-6}T^3-6.43\times10^{-4}T^2+$$
$$+4.88\times10^{-1}T+439.80. \quad (31)$$

The approximation of the physical properties was made using data from [28], the coefficient of determination of the two functions obtained being $r^2\cong1$. The value of the density of P91 steel was assumed to be constant, equal to $\varrho=7750$ kg/m$^3$, as it changes very little in the temperature range for which the calculations were carried out.

Firstly, the temperature distribution in the pipeline wall was determined using a direct, analytical method, with the assumption that the temperature of the fluid increases stepwise from 20°C to 100°C with a heat transfer coefficient at the inner surface of the pipeline of $h=1\,000$ W/(m$^2$K). The transient temperature waveforms were determined at 51 evenly spaced nodes over the wall thickness, where the first node is on the internal surface, and the last node is on the external surface, assuming ideal heat insulation on the external surface of the pipeline ($\dot{q}=0$). In addition, the heat flux and thermal stresses on the inner surface of the pipeline without holes were determined. The temperature waveforms from the selected nodes were then perturbed with random errors and were used as 'measured data' for the calculations performed using the inverse marching method.

Then, the temperature, heat flux and thermal stress on the inner surface were reconstructed using an inverse marching method based on a temperature measurement inside the pipeline wall disturbed by random errors.

In the proposed inverse marching method to monitor thermal stresses in simple shaped elements based on the measurement of the wall temperature at a single point, the sequence of operations is as follows. For a given time, the temperature distribution in the direct area is determined from the temperature measurement at node $N$ and for the insulated outer surface, including the temperature at node $(N+1)$ located at a distance $\Delta r$ from $N$. Then, based on the temperature waveforms at nodes $N$ and $(N+1)$, the temperatures in the inverse region at nodes $(N-1)$, $(N-2)$,..., 1 are determined with a spatial step $\Delta r$, as well as the thermal stress and heat flux at node 1 (on the internal surface).

In the research presented in this paper, the main objective is to evaluate the influence of the number of nodes in the inverse region, the distance of node $N$ from the inner surface and the size of the time step on the accuracy of the performed calculations using the proposed inverse method. Therefore, in the calculations made with the inverse method, the above-described sequence of operations was shortened and the 'measured data' generated by the analytical direct method at nodes $N$ and $(N+1)$ were used immediately.

Cases where the node is located at distances $\delta$ of 6, 12 and 18 mm were analysed. In addition, the inverse area was divided into 2, 3 and 4 control volumes in each case. Calculations were performed for time steps $\Delta t$ with values of 1, 2, 3, 4, 5 and 6 s.

The division of the inverse region in the cross-section of the cylindrical element into finite volumes is shown in Fig 3.

For each case, the mean squared errors of the calculated values of temperature and thermal stresses were determined relative to those determined from the solution of the direct problem. The results of the calculations are shown in Table 1. For each time step, the smallest mean squared error values for a given distance $\delta$ from the internal surface are highlighted in green in Table 1.

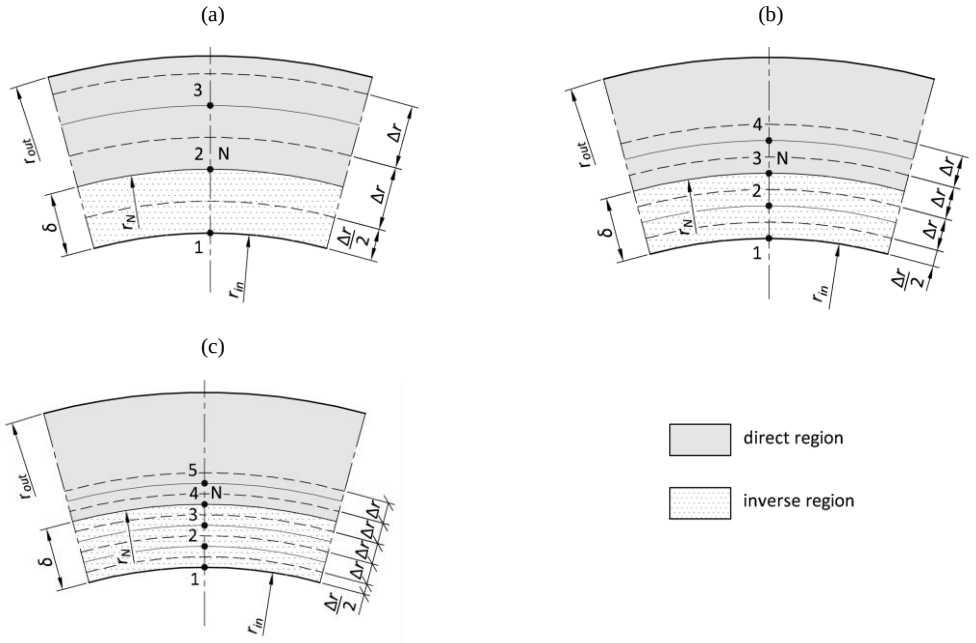


Fig. 3. Division of the inverse area in the cross-section of a cylindrical element into: (a) two control volumes, (c) three control volumes, (c) four control volumes; *N* - position of the wall temperature measurement point.

Table 1. Summary of mean square error values for the determined temperature and thermal stress depending on the value of the time step $\Delta t$, the number of control volumes and the distance from the inner surface $\delta$.

| Number of control volumes | Time step $\Delta t$, s | Distances of the measuring point from the inner surface $\delta$ | | | | | |
|---|---|---|---|---|---|---|---|
| | | 6 mm | | 12 mm | | 18 mm | |
| | | $s_{N,temp}$, K | $s_{N,stresses}$, MPa | $s_{N,temp}$, K | $s_{N,stresses}$, MPa | $s_{N,temp}$, K | $s_{N,stresses}$, MPa |
| 2 | 1 | **0.289** | **0.871** | 0.804 | 2.327 | 1.777 | 4.895 |
| 3 | | 0.344 | 1.040 | 0.761 | 2.271 | 2.632 | 7.744 |
| 4 | | 0.456 | 1.376 | 0.743 | 2.212 | 2.309 | 6.937 |
| 2 | 2 | 0.310 | 0.938 | 0.427 | 1.240 | 0.965 | 2.702 |
| 3 | | 0.373 | 1.131 | 0.469 | 1.373 | 0.887 | 2.567 |
| 4 | | 0.459 | 1.390 | 0.541 | 1.577 | 0.834 | 2.424 |
| 2 | 3 | 0.378 | 1.144 | **0.411** | **1.197** | 0.740 | 2.116 |
| 3 | | 0.417 | 1.268 | 0.502 | 1.472 | 0.660 | 1.898 |
| 4 | | 0.509 | 1.542 | 0.585 | 1.705 | 0.708 | 2.025 |
| 2 | 4 | 0.435 | 1.318 | 0.508 | 1.473 | 0.628 | 1.824 |
| 3 | | 0.477 | 1.448 | 0.594 | 1.743 | 0.670 | 1.922 |
| 4 | | 0.567 | 1.720 | 0.664 | 1.939 | 0.735 | 2.090 |
| 2 | 5 | 0.483 | 1.463 | 0.615 | 1.783 | **0.597** | **1.760** |
| 3 | | 0.522 | 1.584 | 0.671 | 1.972 | 0.719 | 2.064 |
| 4 | | 0.597 | 1.809 | 0.716 | 2.097 | 0.777 | 2.216 |
| 2 | 6 | 0.519 | 1.571 | 0.715 | 2.071 | 0.623 | 1.825 |
| 3 | | 0.543 | 1.651 | 0.731 | 2.154 | 0.776 | 2.236 |
| 4 | | 0.613 | 1.860 | 0.756 | 2.227 | 0.823 | 2.362 |

The best results were obtained for the position of the temperature measuring point at a distance of 6 mm from the inner surface, for which the smallest errors correspond to a time step $\Delta t$ of 1 s and a division into 2 control volumes. For this case, the mean-square error of the temperature $s_{N,temp}$ determined by the inverse marching method is only 0.289 K and the error in determining the thermal stress $s_{N,stresses}$ is 0.871 MPa. For a measuring point distance $\delta$ of 12 mm from the inner surface, the smallest errors are obtained for a time step $\Delta t$ of 2 s and division into 2 control volumes, and for a distance $\delta$ of 18 mm – for a time step $\Delta t$ of 5 s and division also into 2 control volumes. It is not a rule that, for a given time step, a division into two control volumes is the most favourable, especially for smaller time step values, but in fact, the most favourable choice of time step length corresponds to a division into the minimum number of control volumes.

It should also be noted that very large mean squared errors were obtained for $\delta$ = 18 mm and a time step $\Delta t$ of 1 s. These results should not be taken into account because, according to the condition described in Eq. (13), the minimum time step for this distance is 2 s.

The temperature and thermal stress curves calculated by the direct and inverse method on the surface of the analysed thick-walled cylindrical element for several selected cases summari-

sed in Table 1 are shown in Figs. 4 – 9. In the figures, two cases each for distance $\delta$ with, respectively, the smallest and largest mean square error of the determined temperature and thermal stresses using the inverse method are selected.

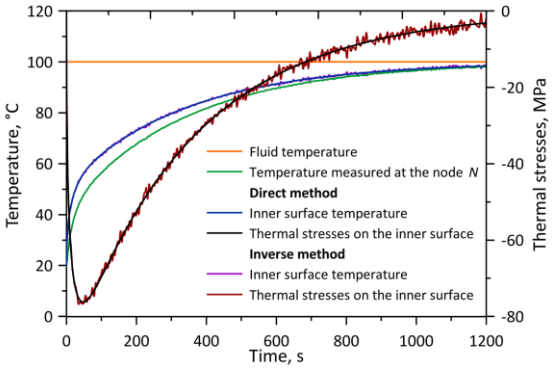


Fig. 4. Results of calculations of temperature and thermal stresses on the internal surface of a cylindrical element for measuring point $N$ at a distance of $\delta = 6$ mm using the direct and inverse method for $\Delta t = 1$ s and division of the inverse area into 2 control volumes.

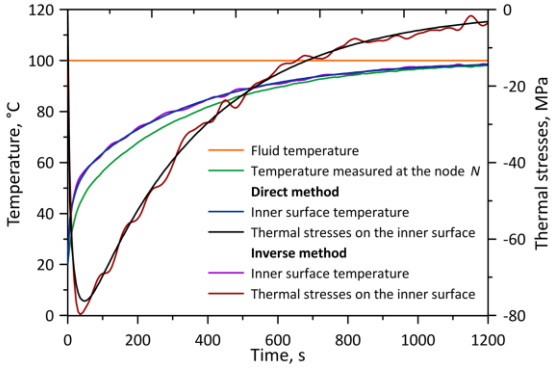


Fig. 5. Results of calculations of temperature and thermal stresses on the internal surface of a cylindrical element for measuring point $N$ at a distance of $\delta = 6$ mm using the direct and inverse method for $\Delta t = 6$ s and division of the inverse area into 4 control volumes.

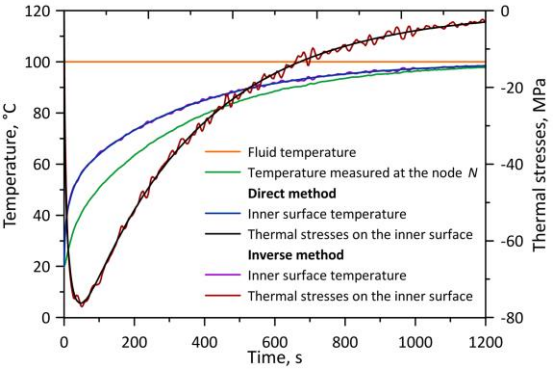


Fig. 6. Results of calculations of temperature and thermal stresses on the internal surface of a cylindrical element for measuring point $N$ at a distance of $\delta = 12$ mm using the direct and inverse method for $\Delta t = 3$ s and division of the inverse area into 2 control volumes.

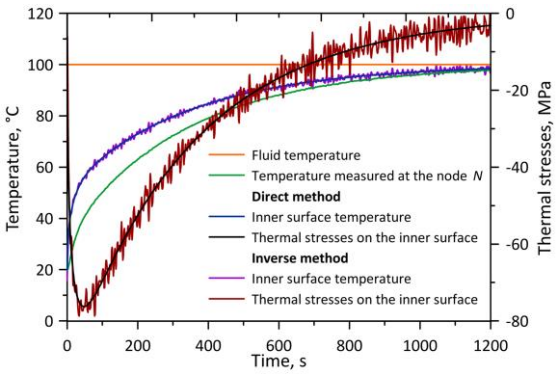


Fig. 7. Results of calculations of temperature and thermal stresses on the internal surface of a cylindrical element for measuring point $N$ at a distance of $\delta = 12$ mm using the direct and inverse method for $\Delta t = 1$ s and division of the inverse area into 2 control volumes.

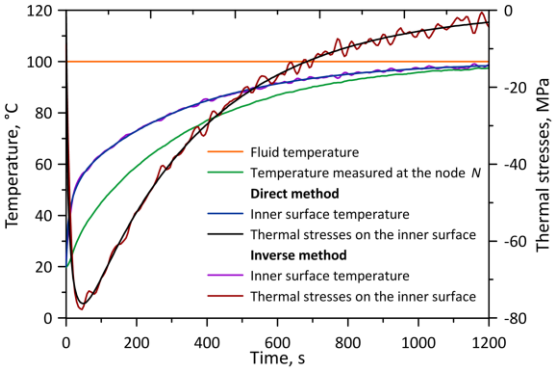


Fig. 8. Results of calculations of temperature and thermal stresses on the internal surface of a cylindrical element for measuring point $N$ at a distance of $\delta = 18$ mm using the direct and inverse method for $\Delta t = 5$ s and division of the inverse area into 2 control volumes.

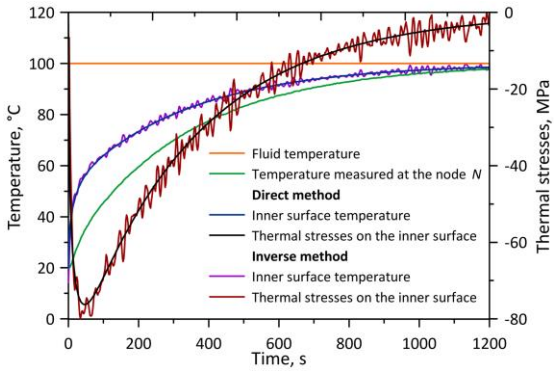


Fig. 9. Results of calculations of temperature and thermal stresses on the internal surface of a cylindrical element for measuring point $N$ at a distance of $\delta = 18$ mm using the direct and inverse method for $\Delta t = 2$ s and division of the inverse area into 2 control volumes.

## 6. Conclusions

Based on analyses of the accuracy of the inverse marching method used to determine thermal stresses in cylindrical pres-

sure elements without holes, the following conclusions can be drawn:

- the best choice of time step length and number of control volumes/nodes depends on the location of the measurement point. It is advisable to select the location of the measuring point by making test calculations and checking which time step and number of nodes will give the results with the lowest errors. The results of the test calculations confirm what could be expected, i.e. the closer the measuring point is to the inner surface, the more accurate the results. If the position of the measuring point is imposed in advance, it is worth carrying out test calculations to determine the optimum number of nodes in the inverted area and the length of the time step;
- the mean squared errors for temperature measurements are less than 1 K (for those selected as most favourable for a given distance from the inner surface $\delta$);
- the mean squared errors of the thermal stresses for the most favourable configurations of the number of control volumes and time step length for a given distance $\delta$ range from 0.871 MPa to 2.424 MPa, corresponding to temperature determination errors of 0.289 K to 0.834 K. The maximum thermal stress during pipeline heating is approximately 76 MPa. This shows how important it is to determine the exact temperature distribution in the pipeline wall and to choose the best possible conditions (time step, distance $\delta$ and number of nodes) for making the calculations using the presented inverse method;
- in addition to the calculations described, the heat transfer coefficient $h$ on the internal surface of the pipeline was determined. However, the mean square errors of the heat transfer coefficient determination are substantial. The slightest error was obtained for the case when the time step is $\Delta t = 3$ s, the inverse area is divided into 4 control volumes, and the measuring point is located at a distance $\delta$ of 6 mm and is 215.6 W/(m$^2$K) with a reference value $h$ of 1 000 W/(m$^2$K). This leads to the conclusion that the heat transfer coefficient should be determined either from a correlation for the Nusselt number or by another method, such as that described in [30].

## Acknowledgements

This work was partially funded by the National Science Centre in Poland within the framework of research project no. 2021/43/B/ST8/01170.

## References

[1] Fang, L., Su, F., Kang Z., & Zhu, H. (2024). Finite element (FE) analysis of thermal stress in production process of multi-layer lining ladle. *Case Studies in Thermal Engineering*, 57, 104307. doi: 10.1016/j.csite.2024.104307

[2] Taler, D., Dzierwa, P., Kaczmarski, K., & Taler, J. (2022). Increase the flexibility of steam boilers by optimisation of critical pressure component heating. *Energy*, 250, 1–18. doi: 10.1016/j.energy.2022.123855

[3] Taler, D., Kaczmarski, K., Dzierwa, P., Taler, J., & Trojan, M. (2024). Optimisation of the cooling of pressurised thick-walled components operating with fluid at saturation temperature. *Energy*, 290, 1–15. https://doi.org/10.1016/j.energy.2023.129975

[4] Oh, Ch., Lee,S., Jhung, M. J., & Huh N.-S. (2022). Analytical approach to estimate the thermal stress distribution of reactor pressure vessel nozzle corners with a constant cooldown rate. *International Journal of Pressure Vessels and Piping*, 197, 104608. doi: 10.1016/j.ijpvp.2022.104608

[5] Jeong, S.-H., Chung, K.-S., Ma, W.J., Yang, J.S., Choi, J.B., & Kim, M. K. (2022). Thermal stress intensity factor solutions for reactor pressure vessel nozzles. *Nuclear Engineering and Technology*, 54, 2188–2197. doi: 10.1016/j.net.2022.01.006

[6] Olivera, S. J., Mostafavia, M., Hosseinzadehb, F., & Paviera, M. J. (2019). Redistribution of residual stress by thermal shock in reactor pressure vessel steel clad with nickel alloy. *International Journal of Pressure Vessels and Piping*, 169, 37–47. doi: 10.1016/j.ijpvp.2018.11.007

[7] Radin, Y.A., Kontorovich, T.S., & Golov, P.V. (2020). Monitoring The Thermal Stress State In Steam Turbines. *Power Technology and Engineering*, 53(6), 719–723. doi: 10.1007/s10749-020-01146-6

[8] Radin, Y.A., & Kontorovich, T.S. (2021). Influence Of The Arrangement Of The Highand Intermediate-Pressure Cylinders Of Steam Turbines With Different Bypass Circuits On Their Thermal Stress State During Start-Ups And Shutdowns. *Power Technology and Engineering*, 54(5), 720–725. doi: 10.1007/ s10749-020-01276-x

[9] Radin, Y.A., & Kontorovich, T.S. (2024). Influence Of Parameter Deviations Vis-À-Vis Assignment Schedule On Thermally Stressed State Of Main Thermal Power Plant Equipment. *Power Technology and Engineering*, 57(6), 918–921. doi: 10.1007/s10749-024-01758-2

[10] Taler, J., Taler, D., Kaczmarski, K., Dzierwa, P., Trojan, M., & Jaremkiewicz, M. (2018). Allowable Rates of Fluid Temperature Variations and Thermal Stress Monitoring in Pressure Elements of Supercritical Boilers. *Heat Transfer Engineering*, 40(17–18), 1430–1441. doi: 10.1080/01457632.2018.1474584

[11] Wacławiak, K., & Okrajni, J. (2019). Transient heat transfer as a leading factor in fatigue of thick-walled elements at power plants. *Archives of Thermodynamics*, 40(3), 43–55. doi: 10.24425/ather.2019.129549

[12] Taler, J., Dzierwa, P., Jaremkiewicz, M., Taler, D., Kaczmarski, K., & Trojan, M. (2018). Thermal stress monitoring in thick-walled pressure components based on the solutions of the inverse heat conduction problems. *Journal of Thermal Stresses*, 41(10−12), 1501–1524. doi: 10.1080/01495739.2018.1520621

[13] Teixeira Júnior, M., Zilio, G., Mortean, M.V.V., de Paiva, K.V., & Oliveira, J.L.G. (2023). Experimental and numerical analysis of transient thermal stresses on thick-walled cylinder. *International Journal of Pressure Vessels and Piping*, 202, 104884. doi: 10.1016/j.ijpvp.2023.104884

[14] Taler, J., & Duda, P. (2000). Experimental verification of space marching methods for solving inverse heat conduction problems. *Heat and Mass Transfer*, 36, 325–331. doi: 10.1007/s002310000082

[15] Jaremkiewicz, M., Dzierwa, P., Taler, D., & Taler, J. (2019). Monitoring of transient thermal stresses in pressure components of steam boilers using an innovative technique for measuring the fluid temperature. *Energy*, 175, 139–150. doi: 10.1016/j.energy.2019.03.049

[16] Jaremkiewicz, M., Taler, D., Dzierwa, P., & Taler, J. (2019). Determination of transient fluid temperature and thermal stresses in pressure thick-walled elements using a new design thermometer. *Energies*, 12, 1–21. doi: 10.3390/en12020222

[17] Taler, J., Dzierwa, P., Jaremkiewicz, M., Taler, D., Kaczmarski, K., Trojan, M., Węglowski, B., & Sobota, T. (2019). Monitoring of transient 3D temperature distribution and thermal stress in pressure elements based on the wall temperature measurement. *Journal of Thermal Stresses*, 42, 698–724. doi: 10.1080/01495739.2019.1587328

[18] Taler, J., Dzierwa, P., Jaremkiewicz, M., Taler, D., Kaczmarski, K., Trojan, M., & Sobota, T. (2019). Thermal stress monitoring in thick walled pressure components of steam boilers. *Energy*, 175, 645–666. doi: 10.1016/j.energy.2019.03.087

[19] Joachimiak, M., Joachimiak, D., & Ciałkowski, M. (2022). Investigation on Thermal Loads in Steady-State Conditions with the Use of the Solution to the Inverse Problem. *Heat Transfer Engineering*, 44(11–12), 963–969. doi: 10.1080/01457632.2022.2113451

[20] Joachimiak, M., & Joachimiak, D. (2024). Stabilization of boundary conditions obtained from the solution of the inverse problem during the cooling process in a furnace for thermochemical treatment. *International Journal of Heat and Mass Transfer*, 224, 125274. doi: 10.1016/j.ijheatmasstransfer.2024.125274

[21] Ciałkowski, M., Joachimiak, M., Mierzwiczak, M., Frąckowiak, A., Olejnik, A., & Kozakiewicz, A. (2023). The analysis of the stability of the Cauchy problem in the cylindrical double-layer area. *Archives of Thermodynamics*, 44(4), 563–579. doi: 10.24425/ather.2023.149735

[22] Taler, J. (1995). *Theory and practice of identifying heat transfer processes*, Zakład Narodowy im. Ossolińskich (in Polish).

[23] TRD 301 (2001). *Zylinderschalen unter innerem Überdruck. Technische Regeln für Dampfkessel (TRD)*, Heymanns Beuth Köln-Berlin.

[24] European Standard EN 12952-3 (2001). *Water-tube boilers and auxiliary installations. Part 3: design and calculation for pressure parts*. European Committee for Standardization.

[25] Taler, J., Dzierwa, P., & Taler, D. (2011). Optimisation of heating and cooling of thick-walled boiler components. In *Thermal and flow processes in large power boilers, Modelling and monitoring* (pp. 584–625). Wydawnictwo Naukowe PWN (in Polish).

[26] Taler, J., & Zima, W. (1999). Solution of inverse heat conduction problems using control volume approach. *International Journal of Heat and Mass Transfer*, 42, 1123–1140. doi: 10.1016/S0017-9310(98)00280-4

[27] Taler, J., Zima, W., & Jaremkiewicz, M. (2016). Simple method for monitoring transient thermal stresses in pipelines. *Journal of Thermal Stresses*, 39, 386–397. doi: 10.1080/01495739.2016.1152109

[28] Taler, J., & Duda, P. (2006). *Solving Direct and Inverse Heat Conduction Problems*, Springer.

[29] Taler, J.(1999). A new space marching method for solving inverse heat conduction problems. *Forschung im Ingenieurwesen*, 64, 296–306. doi: 10.1007/PL00010844

[30] Jaremkiewicz, M., & Taler, J. (2018). Measurement of Transient Fluid Temperature in a Pipeline. *Heat Transfer Engineering*, 39(13–14), 1227–1234. doi: 10.1080/01457632.2017.1363631